Symmetry crossover and excitation thresholds at the neutral-ionic transition of the modified Hubbard model

Y. Anusooya-Pati and Z. G. Soos
Department of Chemistry, Princeton University, Princeton, New Jersey 08544

A. Painelli
Dipartimento Chimica G.I.A.F., Universita' di Parma, I-43100 Parma, Italy

(Received 12 September 2000; published 8 May 2001)

Exact ground states, charge densities, and excitation energies are found using valence bond methods for N-site modified Hubbard models with uniform spacing. At the neutral-ionic transition (NIT), the ground state has a symmetry crossover in $4n$ and $4n+2$ rings with periodic and antiperiodic boundary conditions, respectively. Large site energies Δ stabilize a paired state of the half-filled chain, while large U stabilizes a covalent state. Finite-transfer integrals t shift the NIT to the covalent side of $U-2\Delta$. Exact results to $N=16$ in the full basis and to $N=22$ in a restricted basis for large U and Δ are extrapolated to obtain the crossover and charge density of extended chains. The modified Hubbard model has a continuous NIT between a diamagnetic band insulator on the paired side and a paramagnetic Mott insulator on the covalent side. The singlet-triplet (ST), singlet-singlet (SS), and charge gaps for finite N indicate that the ST and SS gaps close at the NIT with increasing U, and that the charge gap vanishes only there. Finite-N excitations constrain all singularities to $\pm 0.1t$ of the symmetry crossover. The NIT is interpreted as a localized ground state (GS) with finite gaps on the paired side and an extended GS with vanishing ST and SS gaps on the covalent side. The charge gap and charge stiffness indicate a metallic GS at the transition that, however, is unconditionally unstable to dimerization. Finite Δ breaks electron-hole (e-h) symmetry, but the modified Hubbard model has an extended e-h symmetry, and a strong mixing of spin and charge excitations is limited to a few t's about the NIT. Exact finite-size results complement other approaches to valence or ferroelectric transitions in organic charge-transfer salts or in inorganic oxides, and to electron-vibration coupling and structural instabilities in one-dimensional systems.

DOI: 10.1103/PhysRevB.63.205118 PACS number(s): 71.30.+h, 71.10.Fd, 71.27.+a

I. INTRODUCTION

McConnell and co-workers[1] explained the sharp separation of organic charge-transfer (CT) complexes into diamagnetic and paramagnetic by proposing that weak π donors (D) and acceptors (A) form neutral complexes of molecules, while strong donors and acceptors crystallize as ion radicals D^+ and A^-. These planar conjugated systems form one-dimensional structures, either as mixed $\ldots DADA \ldots$ stacks in CT complexes or as segregated stacks in ion-radical salts.[2] The simplest approximation for a crossover between DA and D^+A^- ground states is $M=E_I-E_A$, where M is the Madelung energy, E_I is the ionization potential of the donor, and E_A is the electron affinity of the acceptor. Although M is inherently long ranged, the systems are quasi-one-dimensional by virtue of π-overlap restricted to stacks. Strebel and Soos[3] introduced the modified Hubbard model with transfer integral $t=-\langle DA|H|D^+A^-\rangle$ for CT complexes, and studied the crossover in the random-phase approximation. Finite t leads to mixing and to partial ionicity $D^{\rho+}A^{\rho-}$ in the ground state (GS), with $\Delta\rho<1$ at the crossover. The modified Hubbard model, Eq. (1) below, has proved to be extremely rich and widely applicable. It describes any valence transition, is a special case of important solid-state models, and provides the starting point for electron-phonon (e-ph) coupling. Its scope is still growing and attracting new theoretical and computational approaches to the crossover region, $M\sim E_I-E_A$. In this paper we present exact solutions of finite-size systems, including low-lying excitations.

The neutral-ionic transition (NIT) originates with the TTF-CA complex studied by Torrance,[4] where D is tetrathiafulvalene and A chloranil. TTF-CA is neutral at room temperature, with $\rho\sim 0.3$, and has a transition at $T\sim 81$ K to an ionic state with $\rho\sim 0.7$ that, moreover, is dimerized. The uniform TTF-CA spacing above 81 K becomes alternating ($\ldots t_1,t_2 \ldots$) in the ionic phase, and a partial ionicity is determined spectroscopically.[5] The structural change shows the fundamental role of lattice phonons and a Peierls instability of the paramagnetic phase. The alternating phase is potentially ferroelectric, and the system may be metallic at the NIT. Such features are common to ferromagnetic oxides, and in this context they were recently discussed[6] in terms of the modified Hubbard model. The interplay of electron-electron (e-e) and e-ph interactions can generate either continuous or discontinuous ionicity changes. Long-range Coulomb interactions can generate[7–9] discontinuous ρ variations at the NIT, as well as strongly affect[9] the dimerization instability.

Rice[10] pointed out the strong infrared activity of totally symmetric molecular vibrations through coupling to charge fluctuations. These on-site (Holstein) phonons also participate in the NIT. They condense at the transition, and produce discontinuous ρ variations above a critical coupling

strength.[9] Electron-molecular-vibration coupling provides the basis for a spectroscopic determination of the ionicity ρ of the $D^{\rho+}A^{\rho-}$ GS as well as of the local symmetry, making vibrational spectroscopy an useful tool to follow charge and structural phase transitions.[11] Joint theoretical and experimental analysis of electronic and vibrational spectra[12] allowed for a systematic characterization of several salts.[13]

The modified Hubbard model adds site energies $\pm\Delta$ to a Hubbard chain with uniform spacing:

$$H_0(t,\Delta,U) = -\sum_{i,\sigma} \{t(a^+_{i,\sigma}a_{i+1,\sigma} + a^+_{i+1,\sigma}a_{i,\sigma}) - \Delta(-1)^i a^+_{i,\sigma}a_{i,\sigma}\} + \sum_i U a^+_{i,\alpha}a^+_{i,\beta}a_{i,\beta}a_{i,\alpha} \tag{1}$$

D and A are at odd and even i, respectively, in the context of CT complexes, and $t>0$ and $\Delta \geqslant 0$ can be taken without loss of generality. The half-filled case, with one electron per site, is by far the most important. We consider H_0 at this filling for uniform t and equal $U \geqslant 0$ for donors and acceptors. The electron density on D sites is related to the GS energy:

$$n_D - 1 = -\frac{1}{N}\frac{\partial E_0(t,\Delta,U)}{\partial \Delta}. \tag{2}$$

The ground states of extended systems are not known exactly for $\Delta \neq 0$. Approximate solutions beyond the mean field have been proposed along several lines: exact diagonalization,[7–9,14] quantum Monte Carlo,[15] renormalization-group methods,[16] and continuum models.[17] There is broad agreement as well as open or disputed points mentioned below.

Hubbard models are readily generalized, and provide a unified approach to quantum cell models that need not be low dimensional. In the context of Eq. (1), we note that Δ can incorporate the Madelung energy in a mean-field approximation[3] or coupling to Holstein phonons in the adiabatic approximation.[9,14] In either case, the effective Δ depends on the GS ionicity, and the NIT becomes discontinuous above a critical coupling. The model is then nonlinear, and has wider applications to susceptibilities.[18] At $\Delta=0$, if t is linearly expanded around the equilibrium bond length, we obtain a Peierls-Hubbard model,[19] and a direct connection to models for ion-radical salts such as TTF-TCNQ with segregated stacks. Alternating transfer integrals $t(1\pm\delta)$ are found on the ionic side[2] in many segregated stacks and in conjugated polymers.[20,21] Theoretical interest in $H_0(t,\Delta,U)$ and its variants lies in the interplay of e-e and e-ph interactions and their role in the structural instabilities of one-dimensional materials, broadly defined.[19–22]

The $t=0$ GS of the Hamiltonian in Eq. (1) is sketched in Fig. 1 to illustrate some basic features. The electrons are paired on D (odd) sites for $\Delta > U/2$, paired on A (even) sites for $\Delta < -U/2$, and singly occupy all sites in between; covalent states have $n_i=1$ at all i, and a spin degeneracy of 2^N. The valence transitions at $U=\pm 2\Delta$ for $U>0$ transfer one electron in the GS and $\rho = 2-n_D$ changes discontinuously.

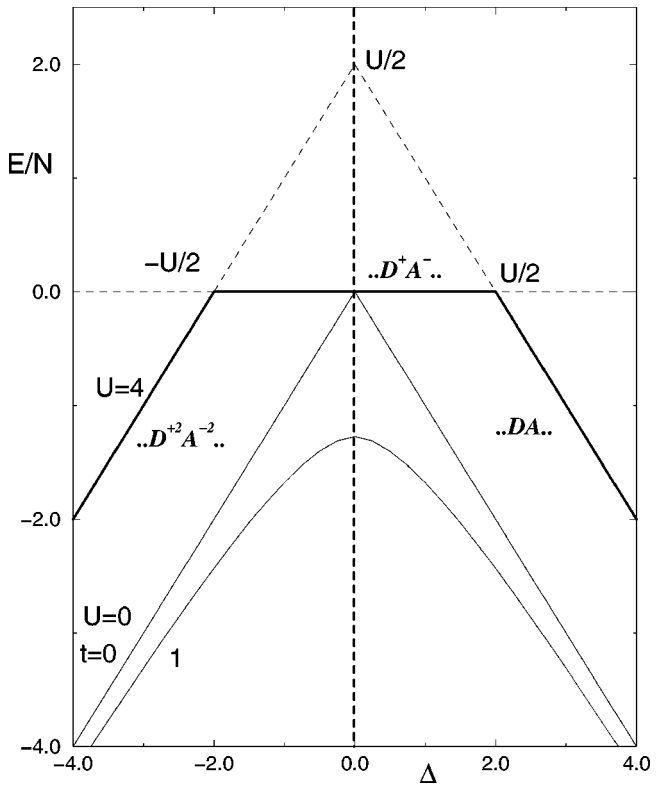

FIG. 1. Ground-state energy per site, E/N, of the modified Hubbard model [Eq. (1)], as a function of the site energy Δ for free ($U=0$) or interacting ($U>0$) electrons in the limit of no overlap ($t=0$), with valence transitions at $\Delta=\pm U/2$ in donor-acceptor stacks. The $t=1$ curve for free electrons is Eq. (3).

Since the paired GS's in Fig. 1 are nondegenerate, we expect finite gaps for spin, optical, and charge carrying excitations. The covalent GS, on the other hand, has vanishing spin gaps.

$H_0(t,\Delta,U)$, with finite t, is a one-dimensional metal at $\Delta=U=0$, a band insulator for $\Delta>0$ and $U=0$, and a Hubbard model for $\Delta=0$ and $U>0$. Finite t leads to continuous n_D at the NIT when Δ is not a function of n_D. Although the ionicity is continuous, the NIT between band and Mott insulators is a true quantum phase transition at $T=0$ K as signaled by the closing of triplet[23] and singlet[8,9] gaps and by the unconditional instability[8,9] to dimerization on the covalent side. The nature of the transition between two insulators has revived interest in the modified Hubbard model in connection with localization and conductivity in correlated systems.[24] Strong charge fluctuations induced by lattice motion[6,24] and related structural instabilities[25] have been rediscovered and underlined. Finite t generates correlated states of the Hamiltonian in Eq. (1) that differ fundamentally from the $t=0$ limit. In spite of sustained research,[6–9,14–16,24–30] no definitive picture has emerged for the $T=0$ K phase diagram of the simple model in Eq. (1).

We present in this paper exact solutions of $H_0(t,\Delta,U)$ for finite N using valence bond (VB) methods[31] that were originally developed[7] for CT complexes. The total spin S is conserved in all versions of Eq. (1). VB diagrams with specified pairing of sites with $n_i=1$ form a large but complete basis for any N. The scope of finite-N results is decisively ex-

tended by using both periodic and antiperiodic boundary conditions and the symmetries of H_0. The oligomers in Sec. II reach $N=16$ in the full basis or $N=22$ in a restricted basis without D^{2+} or A^{2-} sites, compared to $N\sim 10$ in previous studies. Exact excitations near the NIT are related in Sec. III to the opening of gaps, and interpreted as due to localization on the paired side. The GS is metallic at the NIT according to the charge gap and charge stiffness. The NIT marks the boundary between a localized GS for $\Delta \gg U$, and a delocalized GS with vanishing excitation energies as in Hubbard models at $\Delta=0$. We shall briefly mention the role of *e*-ph coupling and intersite *e*-*e* interactions, but defer detailed analysis to subsequent publications.

II. SYMMETRY CROSSOVER AND CHARGE DENSITY

We consider GS properties of $H_0(t,\Delta,U)$ at half-filling, one electron per site, and uniform $t=1$. General solutions of the Hamiltonian in Eq. (1) are restricted to finite N, where eigenstates and energies are accessible. Periodic boundary conditions (PBC's) are readily applied to noninteracting ($U=0$) systems, whose GS energy is

$$\frac{E_0(\Delta,0)}{N} = -\frac{1}{N}\sum_{k\ filled} 2(\Delta^2+4\cos^2 k)^{1/2} \rightarrow -\frac{2}{\pi}(\Delta^2+4)^{1/2}E(q). \tag{3}$$

The expression for the infinite chain is shown in Fig. 1; $E(q)$ is a complete elliptic integral of the second kind, with $q^2=4/(\Delta^2+4)$. From Eq. (2), the GS electronic density on D is:

$$n_D(\Delta,0)-1=\frac{2\Delta K(q)}{\pi(4+\Delta^2)^{1/2}}, \tag{4}$$

where K is the complete elliptic integral of the first kind. The divergence of $\partial n_D/\partial\Delta$ at $\Delta=0$ signals an electronic instability. The behavior of finite rings is different, and shows $4n$ and $4n+2$ effects. The wave vector is $k=0,\pm 2\pi/N$, $\pm 4\pi/N$, . . . π. We have energies $\pm\Delta$ at $k=\pi/2$ when $N=4n$, and two electrons for these orbitals. The degeneracy produces an energy cusp at $\Delta=0$; n_D changes discontinuously, and the partial derivative in Eq. (2) is not defined. Finite rings with $N=4n+2$ have nondegenerate GS's at $\Delta=0$, no cusp and finite $(\partial n_D/\partial\Delta)_0$. The $4n$ and $4n+2$ sequences must coincide in the extended chain, and do so according to Eq. (4), with continuous n_D and divergent $(\partial n_D/\partial\Delta)_0$. Exact $U=0$ results illustrate the extrapolation problems encountered in interacting chains.

The full basis of $H_0(t,\Delta,U)$ increases roughly as 4^N with N, and as 3^N when we exclude doubly ionized sites, i.e., two electrons at A sites or two holes at D sites. We use VB methods[31] to reach $N=16$ for the full basis and $N=22$ for the restricted basis. The basis has over 10^7 singlets or 10^9 Slater determinants with $S_z=0$. Exact solution[32,33] of the extended chain is limited to $\Delta=0$, the Hubbard model. The GS is a nondegenerate singlet, the charge gap is finite for $U>0$, and there is spin-charge separation at large U. Finite t and U always lowers the energy in Fig. 1 compared to $t=0$. The greatest changes occur at $\Delta=\pm U/2$, where t cannot be treated as a small parameter.

In C_N symmetry, the GS of the interacting systems transforms as $k'=\pi$ on the covalent side of $4n$ rings, and as $k'=0$ in $4n+2$ rings. Site energies $\Delta>0$ lower the symmetry from C_N to $C_{N/2}$, and yield a charge-density-wave (CDW) GS. The extended system no longer has inversion centers between sites, which corresponds to reflection between sites for finite N, but retains inversion at the sites or, for finite N, reflection σ_v through the sites. With two sites per unit cell, both $k'=0$ and π transform as $k=0$ in the first Brillouin zone. According to reflection through sites, the covalent GS of $4n+2$ rings is even ($\sigma_v=1$, A_1), and that of $4n$ rings is odd ($\sigma_v=-1$, A_2). The GS of $4n$ rings is degenerate at $\Delta_c(U,N)$, where the symmetry switches from A_2 to A_1 with increasing Δ, and this crossover defines the NIT. In addition to PBC's, we use antiperiodic boundary conditions (APBC's) with reversed sign $t_{1N}=-1$ for transfer between 1 and N. This corresponds to $\phi_{n+N}=-\phi_n$ for the on-site wave functions and a periodicity $2N$. In terms of VB diagrams, we modify σ_v for reflection through sites 1 and $N/2+1$ to

$$\sigma' = \sigma_v(-1)^{n_1}, \tag{5}$$

where n_1 is the occupation number of site 1. The APBC GS has $\sigma'=1$ in $4n$ rings for any Δ,U. The GS of $4n+2$ rings have a crossover from $\sigma'=-1$ at small Δ to $\sigma'=1$ at $\Delta>\Delta_c(U,N)$. The subspaces A_1' and A_2' associated with σ' do not coincide with A_1 and A_2. The paired state is unique and even for either PBC's or APBC's. There are two covalent states, the Kekulé diagrams for benzene, with nearest-neighbor pairing of all spins. We define $|K1\rangle$ and $|K2\rangle$ as pairing spins at sites $2i-1$ and $2i$ and $2i$ and $2i+1$, respectively, for all i. The pairing in $|K1\rangle$ is D^+A^-, while the pairing in $|K2\rangle$ is A^-D^+. The combination $|K1\rangle+|K2\rangle$ transforms as A_1 or A_2' for PBC's and APBC's, respectively, while the out-of-phase combination transforms as A_2 or A_1'.

The $U=\Delta=0$ crossover connects electrons paired as $D^{+2}A^{-2}$ or DA in Fig. 1. For $U>0$, the NIT shifts to positive $U-2\Delta_c$ and $t\neq 0$ preferentially stabilizes the paired GS over the covalent GS because the latter has finite probability for adjacent parallel spins that cannot transfer under Eq. (1). The symmetry changes at $\pm\Delta_c(U,N)$ in rings with either PBC's or APBC's. Exact crossovers are shown in Fig. 2 as $U-2\Delta_c(U,N)$ in the $U,\Delta>0$ quadrant for $U=0.5$, 1, 2, 3, 4, 5, and 10; the inset has $U=100$, 200, 300, and ∞, the last one corresponding to the restricted basis. At fixed U and finite N, the crossovers are similar for $4n$ with PBC's and $4n+2$ with APBC's. The dashed line is an extrapolation to the infinite chain discussed below. The covalent region is very narrow and the crossovers merge at $U=0$. The inset shows that $\Delta_c(U,N)$ is nearly constant for $\Delta>5t$.

We plot $\Delta_c(U,N)$ vs N^{-2} in Fig. 3, and find accurate extrapolation at large Δ and U. The difference between $U=300$ and the restricted basis is due to small admixtures of $A^{2-}D^{2+}$ at energy $U+2\Delta$. The extrapolated limit is U

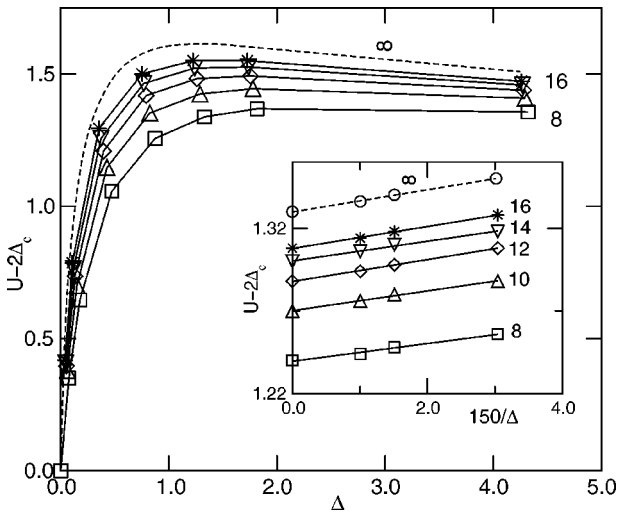

FIG. 2. Ground state crossovers $U(\Delta_c,N)$ of N-site modified Hubbard rings [Eq. (1)] with periodic and antiperiodic boundary conditions, respectively, for $N=4n$ and $4n+2$. The dashed lines are the $N\rightarrow\infty$ extrapolations discussed in the text. The inset shows a large-Δ behavior and the restricted basis at $\Delta\rightarrow\infty$.

$-2\Delta_c=1.332$ in the restricted basis. It has previously been estimated[8] as 1.2–1.3 based on the singlet and triplet gaps, respectively, of $N\leqslant 10$ rings and[23] at 1.5 based on the ionicity up to $N=10$. Mixing with $A^{2-}D^{2+}$ grows as U decreases, as seen for $U=10$, and the functional dependence is closer to $\sim N^{-1}$ at smaller $U\sim 3$. Kinetic contributions are largest at small U and Δ, where t is comparable to CT energies. The extrapolated (dashed) line in Fig. 2 is based on a power law, $\Delta_c(U,N)\propto N^{-\gamma}$, with $1<\gamma<2$ giving the best fit for each U from $N=8$–16.

Figures 2 and 3 indicate that, except for Δ, $U<2t$, the NIT hardly varies with U/Δ. The relevant DA systems have narrow bands, oxides are modeled[6,24] with wider bands, $\Delta<t$. The restricted basis captures the basic physics. We let both Δ and U diverge in $H_0(t,\Delta,U)$ while keeping $\Gamma=\Delta$

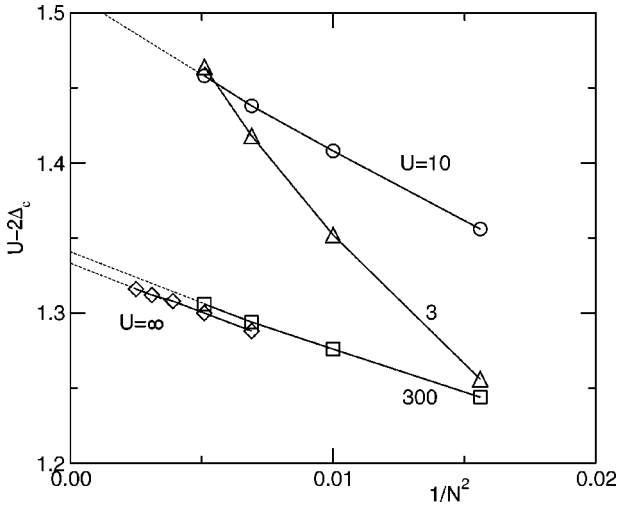

FIG. 3. Size dependence of the GS crossover between $N=8$ and 14 at $U/t=3$, 10, and 300 for the full basis of Eq. (1) and up to $N=20$ in the restricted basis with infinite U.

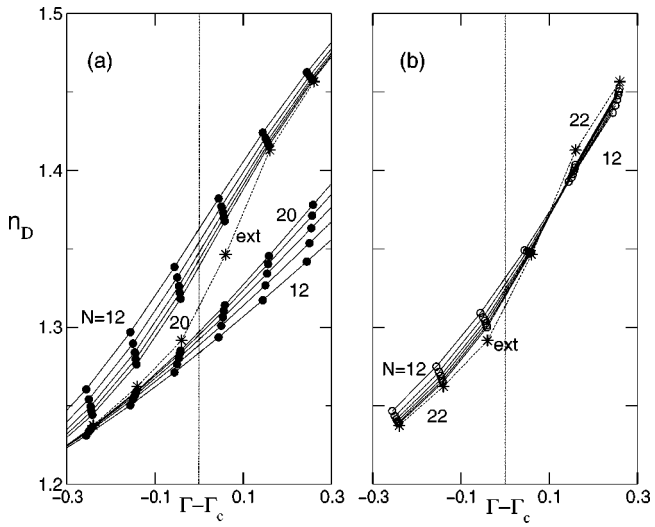

FIG. 4. Ground-state electron density n_D of N-site modified Hubbard rings [Eq. (1)] in the restricted basis. The boundary conditions in (a) produce a symmetry crossover at $\Gamma_c(N)$ (vertical line) where n_D increases discontinuously with Γ and the smallest jump occurs for $N=20$. The boundary conditions in (b), with the same $\Gamma_c(N)$, result in a continuous n_D with increasing $\partial n_D/\partial\Gamma$ up to $N=22$. The stars are joint $N\rightarrow\infty$ extrapolations of (a) and (b) discussed in the text.

$-U/2$ finite,[7] and reference the crossover to $\Gamma-\Gamma_c=\Delta-\Delta_c$. In the half-filled case, $\Delta\rightarrow\infty$ ensures an electron at each D site and excludes two electrons at any A site. The $t=0$ GS has energies -2Γ and 0 per DA on the paired and covalent side, respectively, with $\Gamma=0$ at the NIT. The restricted basis is almost quantitative for $U>5$, makes a larger value of N accessible, and holds at the NIT. The related limit with both U and $U-2\Delta\gg t$ leads instead to a Heisenberg spin chain,[15] without charge degrees of freedom, and does not apply to the NIT.

The GS expectation value, $\langle n_{2i-1}\rangle$, for electrons at D sites is more accurate than the numerical derivative in Eq. (2). Matrix elements[31] over correlated states can be evaluated exactly for finite N. Results for the restricted basis of $4n$ rings with PBC's and $4n+2$ rings with APBC's are shown as a function of $\Gamma-\Gamma_c(N)$ in Fig. 4(a). The crossover generates a jump in n_D. The charge density is continuous in A_1 and A_2 for $4n$ rings, or in A_1' and A_2' for $4n+2$ rings, but continuing the lines in Fig. 4(a) through the NIT gives an excited-state density. All approaches to the NIT described by the Hamiltonian in Eq. (1) indicate n_D to be continuous when t is finite. As expected, the discontinuity in n_D decreases with N, and vanishes in the extended chain. The GS's of $4n+2$ rings with PBC's or $4n$ rings with APBC's remain in A_1 or A_1', respectively, for any U and Δ, and the charge density is continuous, as shown in Fig. 4(b). The NIT defined by the maximum of $\partial n_D/\partial\Delta$ is less precise numerically (by $\sim 0.02t$) than a crossover. The curves in Fig. 4(b) have been adjusted to catch the extrapolation between increasing and decreasing series on either side of Δ_c. Results for the infinite chain are shown as stars that coincide in both panels. They represent joint extrapolations as either N^{-1} or N^{-2}, that give

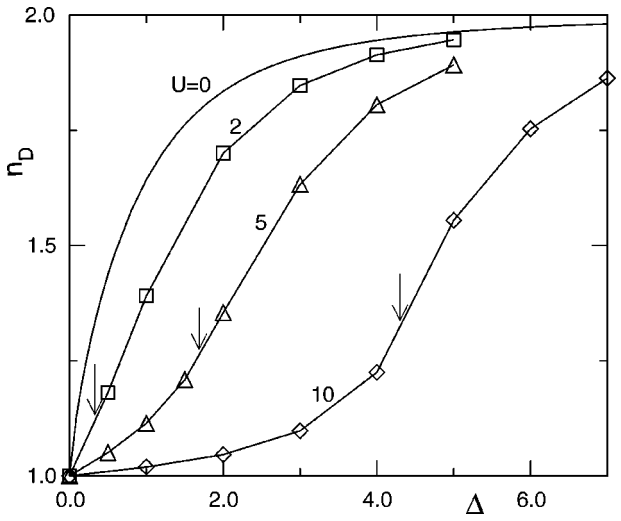

FIG. 5. Ground-state electron density n_D of modified Hubbard models [Eq. (1)], with $U/t=0$, 2, 5, and 10. The exact $U=0$ result is Eq. (4); $U>0$ points are $N\to\infty$ extrapolations of n_D based on the full basis up to $N=16$; the arrows mark the neutral-ionic transition found as in Fig. 3.

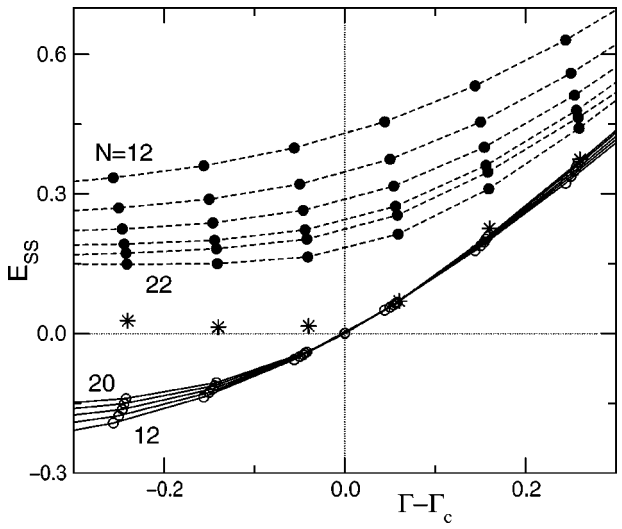

FIG. 6. The singlet-singlet gap E_{SS} near the NIT of Eq. (1) up to $N=22$ in the restricted basis. Boundary conditions leading to crossovers are shown as open circles and $|E_{SS}|$ is the excitation for $\Gamma<\Gamma_c$. Boundary conditions without crossovers are shown as closed circles. The stars are joint $N\to\infty$ extrapolations based on both.

the smallest mean-square deviation. Indeed, n_D is almost quantitatively known from the requirements that $n_D(22)>n_D(20)$ on the covalent side and $n_D(22)<n_D(20)$ on the paired side. The present estimate for n_D is 1.314(2) at the NIT, i.e., $\rho=0.684$.

The restricted basis for $U,\Delta\gg t$ fixes $n_D=1.31$ at the NIT of Eq. (1). The slope $\partial n_D/\partial\Delta$ is finite, but this is inconclusive by itself. Hückel rings show similar $4n$ and $4n+2$ behaviors and exact $N=200$ and 400 results are indistinguishable from n_D in Eq. (4) at the resolution of Fig. 4. The origin must be magnified by an order of magnitude to see the divergence of $\partial n_D/\partial\Delta=(\partial^2 E_0/\partial\Delta^2)/N$ at $\Delta=0$. This divergence signals the intrinsic instability of the $U=\Delta=0$ chain to a site-CDW distortion that, however, is already broken at finite $U=2\Delta_c$ in interacting systems. Extended chains with $U>0$ have finite $\partial n_D/\partial\Delta$ at the NIT. By contrast, the Peierls instability to a bond-CDW is unconditional[9,15] for any t/U, because dimerization breaks reflection symmetry σ_v, as experimentally recognized in the initial TTF-CA studies.[5]

The full basis of the Hamiltonian in Eq. (1) is required for small U, and exact results for n_D or $\Delta_c(U)$ are limited to $N=16$. We again have discontinuous $n_D(\Delta,U)$'s in $4n$ rings with PBC's, and $4n+2$ rings with APBC's, and a continuous n_D for the opposite boundary conditions. In Fig. 5 we compare extrapolated n_D values for $U=2,5$, and 10 with the exact $U=0$ result in Eq. (4). The arrows marking the NIT for finite U are based on symmetry crossovers and extrapolations similar to Fig. 3. We have increasing $n_D(\Delta_c,U)$ with U and the limiting value of ~ 1.3 is reached by $U=5$. Figure 5 shows the stabilization of covalent states with increasing U and small NIT variations for $\Delta,U>2$.

III. ENERGY GAPS AND LOCALIZATION AT THE NIT

The excitations of $H_0(t,\Delta,U)$ provide other evidences of the NIT. The paired and covalent states are diamagnetic and paramagnetic, respectively. A singlet-triplet gap E_{ST} opens[23] at the NIT between a band insulator with $E_{ST}>0$ and a Mott insulator with $E_{ST}=0$. The lowest singlet excitation E_{SS} is between A_1 and A_2 GS; hence E_{SS} vanishes[8] at the NIT. The transition is dipole allowed, and is formally a CT excitation, but E_{SS} rapidly loses oscillator strength on the covalent side. The charge degeneracy in Fig. 1 at $U=2\Delta$, $t=0$ distinguishes between neutral and ionic complexes. The $t>0$ gaps near the NIT are not known, and their simultaneous opening, as tacitly supposed for a single transition,[7–9,14–17] is neither assured nor agreed on.[24–30] We report exact excitation thresholds near the NIT defined by GS crossovers. All symmetry considerations apply to the full basis for $\Delta>0$.

Figure 6 reports $E_{SS}(N)=E_2(N)-E_1(N)$, i.e., the energy difference between A_2 and A_1 GS's, in the restricted basis as a function of $\Gamma-\Gamma_c(N)$. Since $E_{SS}(N)$ increases in $4n$ rings for $\Gamma>\Gamma_c$ and decreases in $4n+2$ rings, we have finite E_{SS} on the paired side. On the covalent side, $E_{SS}(N)$ decreases with N in rings whose GS remains in A_1 or A_1', and increases in rings whose GS is in A_2 or A_2'. Joint extrapolations yield stars that are consistent with vanishing E_{SS} in the extended system. Exact results to $N=22$ in Fig. 6, are the most stringent limits to date, with $E_{SS}<0.05t$ on the covalent side and finite $E_{SS}(N)$ for $\Gamma-\Gamma_c<0.05t$. We note that at $\Delta=0$, far on the covalent side, Ovchinnikov[33] found nonpolar singlets with a zero gap for any $U>0$. Far on the paired side, we have $E_{SS}\sim 2\Gamma$ by inspection. Hence increasing Δ at fixed U in the extended system clearly opens a singlet-singlet (SS) gap that is seen to coincide in Fig. 6, with the NIT defined by the symmetry crossover. The unconditional instability for dimerization on the covalent side is closely related to vanishing E_{SS}; the instability is conditional for a finite gap.

The magnetic gap E_{ST} is to the lowest triplet for either PBC's or APBC's. As shown in Fig. 7, E_{ST} increases rapidly

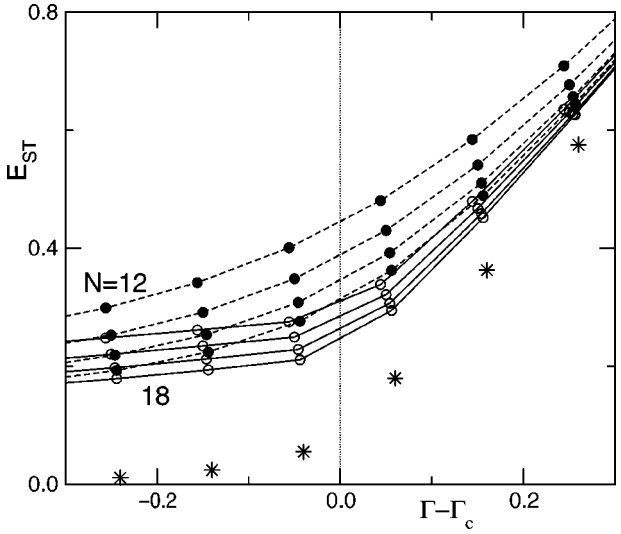

FIG. 7. The singlet-triplet gap E_{ST} near the NIT of Eq. (1) up to $N=18$ in the restricted basis. Open and closed circles refer to boundary conditions with and without crossovers, respectively, and stars are joint $N\rightarrow\infty$ extrapolations based on both.

with $\Gamma>\Gamma_c$ in the restricted basis, and is small on the covalent side. Open circles represent boundary conditions with crossovers and systems whose E_{ST} increases with N at larger $\Gamma-\Gamma_c$. Closed circles are for boundary conditions without crossovers, and show decreasing E_{ST} with N. The stars in Fig. 7 are joint extrapolations. The bound on E_{ST} is $E_{ST}<0.1t$ for $\Gamma<\Gamma_c$, and the gap opens at Γ_c or slightly on the covalent side. At finite U, the extended system is rigorously known to be paramagnetic[34] at $\Delta=0$, with $E_{ST}=0$, and diamagnetic with $E_{ST}\sim 2\Delta-U$ for $\Delta\gg U$. The opening of a singlet-triplet (ST) gap with increasing Δ is assured, and the results in Fig. 7 are consistent with $E_{ST}>0$ at the NIT. The concomitant dimerization on the covalent side opens a magnetic gap, as it is well known in spin chains[2] with regular or alternating exchanges and triplet spin excitons.

The charge gap of the Hamiltonian in Eq. (1) is $I-A$, since there is not an explicit Madelung contribution. $I-A$ is related to the GS of the cation and anion radicals, $E_+(N)$ and $E_-(N)$, respectively, and corresponds to charge disproportionation or electron transfer between noninteracting systems:

$$I(N)-A(N)=E_+(N)+E_-(N)-2E_0(N). \qquad (6)$$

At $t=0$ and $\Delta>0$, we have a paired GS for $U<2\Delta$ with $I=\Delta-U$ and $A=-\Delta$; the lines cross at the NIT, and the covalent side has $I=-\Delta$ and $A=\Delta-U$ for $U>2\Delta$. For $t>0$, the charge gap of free electrons, $|2\Delta|$, follows from the valence and conduction bands in Eq. (3); the extended $U=0$ system is metallic at $\Delta=0$, and insulating otherwise. Although not known exactly for $U>0$, the charge gap is readily shown to be large, roughly $|2\Delta-U|$, far from the NIT. On the covalent side, it becomes the Lieb-Wu gap[32] at $\Delta=0$, and increases as U for $U>4t$; on the paired side, all gaps increase as $2\Delta-U$ for $\Delta\gg U$. Finite N leads to charge gaps at the NIT in systems with discrete energies.

TABLE I. Exact charge gap $I-A$ in Eq. (6), at the neutral-ionic transition of the model in Eq. (1), for rings of N sites, with $t=1$, variable U, and $\Delta_c(N)$ at the crossover of $4n(4n+2)$ rings with periodic (antiperiodic) boundary conditions.

N	$U=2$	10	∞ (restricted basis)
8	0.1893	0.7162	0.8486
10	0.1803	0.6548	0.7614
12	0.1718	0.6010	0.6909
14	0.1614	0.5555	0.6342
16			0.5874
18			0.5469

Both e-h symmetry[35] and σ_b are broken for $\Delta>0$, but their product remains a symmetry operation. Extended e-h symmetry[36] cuts the basis, either full or restricted, roughly in half, and corresponds in the $S=0$ manifold to the $A_g^+\oplus B_u^-$ and $A_g^-\oplus B_u^+$ subspaces of $H_0(t,0,U)$. The GS symmetry does not change at the NIT. e-h symmetry relates the GS and excited states of the radical ions.[35,36] In particular, we have $E_-(N)=E_+(N)+U$, a general result that holds on adding any spin-independent potential to $H_0(t,\Delta,U)$. It follows that Eq. (6) reduces to $I(N)+A(N)=-U$ for even N and arbitrary t,Δ,U. Table I reports $I(N)-A(N)$ at U and Δ_c up to $N=14$ in the full basis and $N=18$ in the restricted basis. The $U=0$ gaps vanish at the crossover, where the electron transfer described in Eq. (6) involves degenerate orbitals. The charge gaps increase with U, but remain small at the crossover even for divergent U. The gaps in Table I follow power laws $N^{-\gamma}$, with $\gamma<0.6$, and place a rough bound of $\sim 0.2t$ on the extended system. The charge gap vanishes at most at a single point, $\Delta_c(U)$ or $U_c(\Delta)$, that coincides with the NIT within the accuracy of finite systems.

The SS, ST, and charge gaps are all finite on the paired side, $\Gamma>\Gamma_c$. They differ on the covalent side, however, where only the charge gap is finite. We associate gaps on the paired side with localization. The GS for the $|\Delta|\gg U$ limit has paired spins on either odd or even sites, and is manifestly localized. Since gapless triplets and singlets are firmly established[33] at $\Delta=0$, the GS of $H_e(t,\Delta,U)$ for $U,t>0$ is extended at $\Delta=0$, and localized at $\Delta\gg U$. A localization-delocalization transition between two insulators incorporates all aspects of the NIT, and the vanishing charge gap suggests a metal at the transition. We develop these ideas below.

To show localization on the covalent side, we partition H_0 in the restricted basis into h_0 for transfers between sites $2n-1$ and $2n$, as in $|K1\rangle$, and a perturbation V for transfers between $2n$ and $2n+1$. We take $\Gamma=\Delta-U/2>0$ in units of t, and solve the 2×2 dimer problem in the singlet subspaces of h_0. The exact GS of h_0 is

$$|G_0(\Gamma)\rangle=\prod_{i=1}^{N/2}\,[a^+_{2i-1,\alpha}a^+_{2i-1,\beta}\cos\phi+\sqrt{2}(a^+_{2i-1,\alpha}a^+_{2i,\beta} - a^+_{2i-1,\beta}a^+_{2i-1,\alpha})\sin\phi]|0\rangle, \qquad (7)$$

where $|0\rangle$ is the vacuum state and $\tan 2\phi=\sqrt{2}/\Gamma$ governs the mixing of $|DA\rangle$ and the singlet linear combination of

TABLE II. Approximate ground-state energy per dimer [Eq. (9)], of the infinite chain, and exact results for Eq. (1) with $N=12$, $t=1$, $\Gamma=\Delta-\Delta_c(12,U)$, and $U=10$, and ∞ (the restricted basis).

Γ	$U=10$, exact	$U=\infty$, exact	$U=\infty$, Eq. (9)
0.5	−2.4706	−2.3757	−2.3148
2.0	−4.8129	−4.7795	−4.7871
5.0	−10.3848	−10.3788	−10.3814
10.0	−20.1981	−20.1971	−20.1975

$|D^+A^-\rangle$. The zeroth-order energy is $-\Gamma-(\Gamma^2+2)^{1/2}$ per dimer. The opposite choice of $2n$ and $2n+1$ for dimers has the same energy but admixes $|A^-D^+\rangle$ singlets, as in $|K2\rangle$. Each dimer has a triplet with excitation energy $\epsilon_T=\Gamma+(\Gamma^2+2)^{1/2}$, a singlet at $\epsilon_S=2(\Gamma^2+2)^{1/2}$, and strictly confined electrons. The perturbation

$$V=-\sum_{i,\sigma}\ (a^+_{2i,\sigma}a_{2i+1,\sigma}+a^+_{2i+1,\sigma}a_{2i,\sigma}) \tag{8}$$

is necessarily small when Γ is large. To second order in V, the energy per dimer is

$$\epsilon^{(0)}+\epsilon^{(2)}=-\Gamma-(\Gamma^2+2)^{1/2}-\frac{\cos^4\phi+(\sin^4\phi/4)}{(\Gamma^2+2)^{1/2}}. \tag{9}$$

Electrons are now confined to adjacent dimers that are connected by virtual excitations. As shown in Table II, Eq. (9) is nearly quantitative as close to the NIT as $\Gamma=2$. Localization to adjacent dimers approximates the exact solution of Eq. (1), which for $N=22$ is a linear combinations of over 10^7 singlets. Rapid convergence with N also points to localization on the paired side, and is seen for n_D in Fig. 4, E_{SS} in Fig. 6, and E_{ST} in Fig. 7. Successive orders in V increase the number of coupled dimers by one. Such an expansion fails at the NIT or on the covalent side.

To see if the system is metallic at the transition, we compute the charge stiffness[37] relevant to the Hamiltonian in Eq. (1). This property has been applied to interacting fermions[38–40] in one dimension. The perturbation is a phase factor $\exp(\pm if)$ in Eq. (1) for transfers to the right and left:[39]

$$V(f)=(1-\cos f)\,\nu_+ + i\,\nu_-\sin f. \tag{10}$$

The first term of Eq. (1) is $-\nu_+$, while ν_- has oppositely signed transfers to the right and left and connects A_1 and A_2 states for PBC's. We now have $E_0(\Gamma,t,f)$ in units of t. The charge stiffness per site is $\chi_{cs}=(\partial^2E_0/\partial f^2)_0/N$. It is finite in conductors, and vanishes in insulators. At the crossover, the proper zeroth-order GS of $4n$ rings is the odd linear combination of the A_1 and A_2 GS's and

$$\chi_{cs}(\Gamma_c)=\left(\frac{\partial^2E_0}{N\partial f^2}\right)_0=p^{(1)}+p^{(2)}$$
$$=\frac{|E_0|}{N}+\frac{\Gamma_c(n_D^{(1)}+n_D^{(2)}-2)}{2}. \tag{11}$$

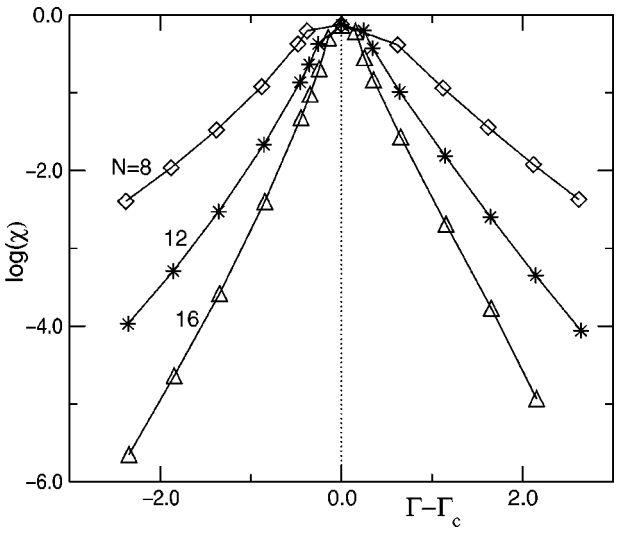

FIG. 8. Charge stiffness, $\chi_{cs}(\Gamma)$ in Eq. (12) and as discussed in the text, near the NIT of the N-site model [Eq. (1)], in the restricted basis; $\chi_{cs}(\Gamma_c)$ is ~60% of the free-fermion value.

Here $n_D^{(1)}$ and $n_D^{(2)}$ are the electron densities at donor sites in the A_1 and A_2 subspaces, respectively, and $p^{(1)}$ and $p^{(2)}$ are the corresponding bond orders, with $2p$ defined as the GS expectation value of ν_+, which we evaluate in the restricted basis. The donor densities at the NIT are shown in Fig. 4 and have opposite N dependences in A_1 and A_2. The value of $\Gamma_c=U/2-\Delta_c=-0.666$ follows from Fig. 3. We have a poor metal: $\chi_{cs}(\Gamma_c)\sim0.74$ is ~60% of $4/\pi$ value for free electrons at $\Delta=U=0$ in Eq. (1). For $\Gamma\neq\Gamma_c$, second-order perturbation theory in f becomes exact.[39] Figure 8 shows that $\chi_{cs}(\Gamma)$ is exponentially small on either side of the NIT. The charge stiffness[38] of the Hubbard model has a similar peak at $U=0$ that narrows with N, and becomes a δ function in the infinite chain. Hence we expect $\chi_{cs}(\Gamma)$ to vanish except at Γ_c in the extended system.

A metallic point connecting insulating phases was recently discussed for $H_0(t,\Delta,U)$,[24] and for the following half-filled system of spinless fermions[40]:

$$H=-\sum_i\ (a_i^+a_{i+1}+a_{i+1}^+a_i)+\sum_i\ (\mathcal{V}n_in_{i+1}+\mathcal{W}n_in_{i+2}). \tag{12}$$

Large $\mathcal{V}>0$ favors a GS without adjacent occupied sites, while large $\mathcal{W}$ favors one with adjacent filled and empty sites along the chain. The $t=0$ crossover occurs at $\mathcal{V}=2\mathcal{W}$, with adjacent electrons and holes for $\mathcal{V}<2\mathcal{W}$ that resemble D and A sites, respectively. The $\mathcal{V}>2\mathcal{W}$ GS has alternating filled and empty sites that, taken in pairs, correspond to D^+ and A^-. The crossover is not precisely at $\mathcal{V}=2\mathcal{W}$, presumably due to different bond orders in the two GS's. It shifts to $\mathcal{W}-\mathcal{V}/2\sim-0.6$ in units of t, very close to Γ_c. Transfers between two sites in Eq. (12) differ from spin degeneracy in Eq. (1), however, and the models do not map into each other. Exact results[40] to $N=40$ for Eq. (12) are comparable to $N=20$ for the full basis of Eq. (1). The striking similarity

between Fig. 8 and the charge stiffness of Eq. (12) up to $N=40$ suggests a similar interpretation.

IV. DISCUSSION

The modified Hubbard model in Eq. (1) has many applications to both theory and experiment. With variations, it is suitable for modeling valence transitions, excitation thresholds, and electronic or structural instabilities, among other topics. Its two parameters U/t and Δ/t encompass the Hubbard model ($\Delta=0$) at half-filling or other filling, two bands at $U=0$, and localized dimers for $\Delta \gg U$. At fixed U and t, increasing $\Delta>0$ generates a neutral-ionic transition whose characterization is the principal goal of this paper. The NIT of the Hamiltonian in Eq. (1) has a continuous ionicity given by Eq. (2) and excitation gaps for singlets, triplets, and charges that are not known exactly. Previous approximations were separately developed for n_D, E_{SS}, E_{ST}, the charge gap, the GS at the NIT, instabilities, etc. Our collective analysis of symmetry crossovers, excitation thresholds, and GS properties incorporates computational advances, and yields better estimates for extended systems.

Finite-size results require extrapolations whose accuracy improves with N. We followed the NIT of $H_0(t,\Delta,U)$ through the symmetry crossover of the GS, the charge density n_D, the excitations E_{SS} and E_{ST}, and the charge gap and stiffness. Larger N is accessible in the restricted basis, allowing for an accurate estimate of $\Gamma_c=-0.666t$ from the crossover and setting stringent limits of $\sim 0.1t$ for the opening of all three gaps at this position. Thus the numerical results point to a single transition. The NIT of the modified Hubbard model is continuous, as previously found, and is marked by the opening of singlet, triplet, and charge gaps on the paired side. There is no gap in the singlet or triplet manifold on the covalent side. The interacting system is known to have a delocalized GS at $\Delta=0$, the Hubbard limit, and a localized GS for $\Delta \gg U$, the paired limit. We identify the NIT at $\pm\Delta_c(U,t)$ as the appearance of a localized GS.

Resta and Sorella[24] discussed polarization and metallic behavior at the NIT in the context of oxides, with $t_0=3.5$ eV, $\Delta'=2.0$ eV and variable U in Eq. (1). The crossover in $N=8$ rings, at $U/t_0=2.27$, is used to estimate the polarization of extended systems. Since $\Delta'/t_0=0.571$ corresponds to large t, the crossover is near the origin of the Δ and U plane in Fig. 2, and there are substantial finite-size effects. The $N=8$ result in Fig. 2 yields $U_c=2.27$, in quantitative agreement with Ref. 24, but larger N's up to 16 extrapolate to larger $U_c/t=2.70$ for the extended system. Such corrections are consistent with $N\sim 10$ results on CT complexes. The GS polarizability is a new approach, to our knowledge, different from the charge stiffness, to the identification of metallic behavior.

The GS density is $n_D=1.314$ at the NIT of the restricted basis, when one electron is always confined to D. The spin degeneracy of D^+ or A^- spoils an exact analysis. The degeneracy of charge and spin excitations at the NIT gives a simple, heuristic interpretation: $n_D=4/3$ is the result for equal weights of molecules and spin-1/2 radical ions. Equal weights at the NIT can be justified rigorously at $U=0$ for electrons or spinless fermions, but not in the restricted basis. We found $\Gamma_c=-0.666$ in the restricted basis and use this value in $|G_0(\Gamma)\rangle$, the dimer GS in Eq. (7); the paired-state amplitude is $\cos^2\phi=0.287$, which corresponds to $n_D=1.287$. Dimers capture most of the configuration mixing of the extended system. The full basis has contributions from D^{2+} and A^{2-} diagrams, which, as seen in Fig. 5, reduce n_D compared to the restricted basis.

Peierls-Hubbard models are widely applied to structural instabilities. The stability of the GS to a perturbation can be formulated in terms of susceptibilities χ that are formally given by the exact eigenstates $|F\rangle$ and energies E_F of the Hamiltonian in Eq. (1). The perturbation is written as the product θQ, where θ is the relevant operator for coupling to Q, and the corresponding χ is

$$\chi \propto -\left(\frac{\partial^2 E_G}{\partial Q^2}\right)_0 = 2\sum_F \frac{|\langle G|\theta|F\rangle|^2}{E_F-E_G}. \tag{13}$$

Since the sum is over the excited states of the unperturbed system, the eigenstates of the uniform chain in Eq. (1) suffice for the stability of the modified Hubbard model. The charge stiffness in Eq. (12) is χ with respect to a magnetic field perpendicular to the ring,[39] and gives information about current flow. Structural transitions are investigated by introducing phonons as the Q perturbation. The Peierls instability for dimerization involves $k=0$ phonons, with θ representing the staggered bond-order operator [the first term in Eq. (1), augmented by a $(-1)^i$ factor]. This operator breaks inversion symmetry at the sites and mixes A_1 and A_2 singlets.[8] Vanishing E_{SS} on the covalent side of the NIT then indicates a divergent χ and the unconditional instability of a lattice with harmonic potentials.[9] On-site (Holstein) phonons couple instead to a CDW operator n_D. Since $\chi_\Delta=\partial n_D/\partial\Delta$ is finite at the NIT, except for $\Delta=0$, the corresponding instability is conditional;[9] the NIT marks the maximum χ_Δ, i.e., the maximum $\partial n_D/\partial\Delta$, as discussed in Fig. 4.

We turn next to open or controversial aspects of the NIT of the modified Hubbard model. Some authors[25,29] proposed two transitions related to the closing of charge and spin gaps, respectively; a spontaneously dimerized phase then separates a band insulator corresponding to the paired GS and Mott insulator on the covalent side.[25] The suggestions[25] for another transition rest on the analogy with spin-1/2 Heisenberg antiferromagnetic chains with frustration due to a second-neighbor exchange J_2. The Kekule diagram $|K1\rangle$ or $|K2\rangle$ is the exact GS at $J_2=J_1/2$, as recognized by Majumdar and Ghosh.[41] There is no exact mapping of Eq. (1) into such a spin chain, not even at large U, but the GS's of related models with, for example, second-neighbor transfers, have not been studied in detail. Our exact results for $H_0(t,\Delta,U)$ with finite N show that the maximum of $\partial\rho/\partial\Delta$, the closing of the singlet and triplet gaps, and the vanishing of the charge gap coincide at the NIT within $\sim 0.1t$. Finite systems cannot specify transitions, but provide some constraints. The Mott insulator dimerizes spontaneously for any t/U, as discussed for the spin-Peierls instability[42] of Heisenberg antiferromagnetic chains. The dimerization amplitude becomes very small

for $U \gg t$ and $J = t^2/U$, since the electronic stabilization is less than J, but the singularity actually increases;[43] the GS energy in Eq. (3) at $U = \Delta = 0$ goes as $\delta^2 \ln \delta$ for alternating $t(1 \pm \delta)$ along the chain, while the GS of the spin chain with alternating $J(1 \pm \delta)$ goes as $\delta^{4/3} \ln \delta$.[44] Such considerations apply to Eq. (1) in the covalent limit $\Gamma = U - 2\Delta \gg t$ where, as noted originally,[1,2] we have a Heisenberg chain with $J = t^2/\Gamma$.

The charge gap is a recent topic, and is expected to have a minimum at NIT.[29,30,45] We find finite minima in interacting systems with finite N. As already noted, the polarizability[24] and charge stiffness in Eq. (12) and Fig. 8 give independent indications of a metallic GS at the NIT. We consequently expect a vanishing charge gap there. The metal separating two insulating phases is extremely fragile: not only is it restricted to a single point $\Delta_c(U)$, but it is unconditionally unstable to dimerization. Moreover, extending the model in Eq. (1) to include intersite e-e interactions or onsite phonons produces a discontinuous NIT above some critical coupling, which excludes a metallic phase even for a rigid lattice. By contrast, a metallic GS at the NIT of Eq. (1) is fairly robust. We have a simple half-filled band at $U = 0$, and a correlated metal persists to an arbitrarily large U. At the NIT, Δ counterbalances U: the charge distributions DA and D^+A^- are almost degenerate, and hence are strongly mixed by any finite t. A metallic state at NIT is not consistent with finite triplet excitation there.

The degeneracy of charge and spin excitations is characteristic of the NIT, and appears already in the $t = 0$ limit of Fig. 1. Finite Δ completely spoils the spin-charge separation at the NIT of Eq. (1). The vanishing E_{ST} is closely linked to the magnetic susceptibility of the Hubbard or Heisenberg chains. Since a singlet can always be constructed from two triplets, a vanishing E_{SS} follows immediately, and is associated with even-parity spin waves in $\Delta = 0$ systems with e-h symmetry. This symmetry is broken in Eq. (1) or its extensions, and the CT excitation connecting the A_1 and A_2 GS's is dipole allowed. Spin-charge separation is regained on the covalent side when the charge gap exceeds a few t, much as in Hubbard models for $U > t$: Exact separation requires infinite U, but $U > 4t$ suffices in practice.

To summarize, we have extended exact solutions of the modified Hubbard model in Eq. (1) to larger systems, identified the NIT with symmetry crossovers in rings with periodic or antiperiodic boundary conditions, and found the charge density, excitation thresholds, and susceptibilities at the NIT. We find a continuous NIT, and considerably tighten the extrapolated limits for the infinite chain. Our results indicate a $T = 0$ K transition with vanishing singlet and triplet gaps on the covalent side, a vanishing charge gap and metallic GS at the NIT, and finite singlet, triplet, and charge gaps on the paired side, whose localized GS is confirmed. We associate the NIT of the model in Eq. (1) with a transition from a delocalized GS (small Δ) to a localized GS (large Δ). An accurate analysis of the Hamiltonian in Eq. (1) is required to model valence transition in charge-transfer salts or metal oxides where long-range Coulomb interactions and e-ph coupling have to be considered explicitly.

ACKNOWLEDGMENTS

One of us (A.P.) thanks A. Girlando for helpful discussions, and J. Voit for exchanging interesting correspondence on the subject and for sharing information on unpublished work. We gratefully acknowledge support for work at Princeton from the National Science Foundation through Grant No. DMR-9530116, and the MRSEC program under Grant No. DMR-9400362, and, for work in Parma from the Italian National Research Council (CNR) within its ''Progetto Finalizzato Materiali Speciali per Tecnologie Avanzate II,'' and by the Ministry of University and of Scientific and Technological Research (MURST).

[1] H.M. McConnell, B.M. Hoffman, and R.M. Metzger, Proc. Natl. Acad. Sci. U.S.A. **53**, 46 (1965); P.L. Nordio, Z.G. Soos, and H.M. McConnell, Annu. Rev. Phys. Chem. **17**, 237 (1966).

[2] Z. G. Soos and D. J. Klein, in *Treatise on Solid State Chemistry*, edited by N. B. Hannay (Plenum, New York, 1976), Vol. III, p. 689.

[3] P.J. Strebel and Z.G. Soos, J. Chem. Phys. **53**, 4077 (1970).

[4] J.B. Torrance, Phys. Rev. Lett. **46**, 253 (1981); **47**, 1747 (1981)

[5] A. Girlando *et al.*, J. Chem. Phys. **79**, 1075 (1983).

[6] T. Egami, S. Ishihara, and M. Tachiki, Science **261**, 1307 (1993); T. Egami and M. Tachiki, Phys. Rev. B **49**, 8944 (1994).

[7] Z.G. Soos and S. Mazumdar, Phys. Rev. B **18**, 1991 (1978).

[8] A. Girlando and A. Painelli, Phys. Rev. B **34**, 2131 (1986).

[9] A. Painelli and A. Girlando, Phys. Rev. B **37**, 5748 (1988); **39**, 9663 (1989).

[10] M.J. Rice, Solid State Commun. **31**, 93 (1979).

[11] A. Painelli and A. Girlando, J. Chem. Phys. **84**, 5655 (1986); R. Bozio and C. Pecile, in *Spectroscopy of Advanced Materials*, edited by R. J. H. Clark and R. E. Hester (Wiley, New York, 1991), Vol. 19, p. 1.

[12] A. Painelli and A. Girlando, J. Chem. Phys. **87**, 1705 (1987).

[13] A. Girlando, A. Painelli, and C. Pecile, Mol. Cryst. Liq. Cryst. **120**, 17 (1985); C. Pecile, A. Painelli, and A. Girlando, *ibid.* **171**, 69 (1989).

[14] A. Painelli and A. Girlando, Phys. Rev. B **45**, 8913 (1992).

[15] N. Nagaosa and J. Takimoto, J. Soc. Jpn. **55**, 2735 (1986); **55**, 2747 (1986); N. Nagaosa, *ibid.* **55**, 2756 (1986).

[16] M. Avignon, Phys. Rev. B **33**, 205 (1986); E.R. Gagliano, C.A. Balseiro, and B. Alascio, *ibid.* **37**, 5697 (1988).

[17] B. Horovitz and J. Solyom, Phys. Rev. B **35**, 7081 (1987).

[18] A. Painelli, Chem. Phys. Lett. **285**, 352 (1998).

[19] A. Painelli and A. Girlando, in *Interacting Electrons in Reduced Dimension*, Vol. 213 of *NATO Advanced Study Institute, Series B: Physics*, edited by D. Baeriswyl and D. K. Campbell, (Plenum, New York, 1989) p. 189; D. Baeriswyl, D. K. Campbell, and S. Mazumdar, in *Conducting Polymers*, edited by H. Kiess (Springer-Verlag, Heidelberg, 1992), p. 7.

[20] *Handbook of Conducting Polymers*, 2nd ed., edited by T. E.

Skotheim, R. L. Elsenbaumer, and J. R. Reynolds (Dekker, New York, 1998).
[21] Z. G. Soos and G. W. Hayden, in *Electroresponsive Molecular and Polymeric Systems*, edited by T. E. Skotheim (Dekker, New York, 1988), p. 197.
[22] *Relaxations of Excited States and Photo-Induced Structural Phase Transitions*, edited by K. Nasu, Springer Series in Solid-State Sciences Vol. 124 (Springer-Verlag, Heidelberg, 1997).
[23] Z.G. Soos, S.R. Bondeson, and S. Mazumdar, Chem. Phys. Lett. **65**, 331 (1979).
[24] R. Resta and S. Sorella, Phys. Rev. Lett. **74**, 4738 (1995); **82**, 370 (1999).
[25] M. Fabrizio, M.O. Gogolin, and A.A. Nersesyan, Phys. Rev. Lett. **83**, 2014 (1999).
[26] G. Ortiz, P. Ordejon, R.M. Martin, and G. Chiappe, Phys. Rev. B **54**, 13 515 (1996).
[27] N. Gidopoulos, S. Sorella, and E. Tosatti, Eur. Phys. J. B **14**, 217 (2000).
[28] S. Caprara, M. Avignon, and O. Navarro, Phys. Rev. B **61**, 15 667 (2000).
[29] Y. Takada and M. Kido, cond-mat/0001239 (unpublished).
[30] S. Qin *et al.*, cond-mat/0004162 (unpublished).
[31] Z. G. Soos and S. Ramasesha, in *Valence Bond Theory and Chemical Structure*, edited by D. J. Klein and N. Trinajstic (Elsevier, New York, 1990), p. 81; G. Wen and Z.G. Soos, J. Chem. Phys. **108**, 2486 (1998).
[32] E.H. Lieb and F.Y. Wu, Phys. Rev. Lett. **25**, 1445 (1968).
[33] A.A. Ovchinnikov, Zh. Éksp. Teor. Fiz. **57**, 2137 (1969) [Sov. Phys. JETP **30**, 1160 (1970)].
[34] M. Takahashi, Prog. Theor. Phys. **42**, 1098 (1969); **43**, 1619 (1970).
[35] A.D. McLachlan, Mol. Phys. **2**, 276 (1959); O.J. Heilmann and E.H. Lieb, Trans. NY Acad. Sci. **33**, 116 (1971); S.R. Bondeson and Z.G. Soos, J. Chem. Phys. **71**, 3807 (1979).
[36] Z.G. Soos, S. Kuwajima, and R.H. Harding, J. Chem. Phys. **85**, 601 (1986).
[37] W. Kohn, Phys. Rev. A **133**, 171 (1964).
[38] B.S. Shastry and B. Sutherland, Phys. Rev. Lett. **65**, 243 (1990); C.A. Stafford, A.J. Millis, and B.S. Shastry, Phys. Rev. B **43**, 13 660 (1991); R.M. Fye, M.J. Martin, D.J. Scalapino, J. Wagner, and W. Hanke, Phys. Rev. B **44**, 6909 (1991).
[39] Z.G. Soos, Y. Anusooya-Pati, and S.K. Pati, J. Chem. Phys. **112**, 3133 (2000).
[40] E.V. Tsiper and A.L. Efros, J. Phys.: Condens. Matter **9**, L561 (1997).
[41] C.K. Majumdar and D.K. Ghosh, J. Math. Phys. **10**, 1388 (1969).
[42] J. W. Bray, L. V. Interrante, I. S. Jacobs, and J. C. Bonner, in *Extended Linear Chain Compounds*, edited by J. S. Miller (Plenum, New York, 1983), Vol. 3, p. 353.
[43] Z.G. Soos and G.W. Hayden, Mol. Cryst. Liq. Cryst. **160**, 421 (1988).
[44] J.L. Black and V.J. Emery, Phys. Rev. B **23**, 429 (1981).
[45] J. Voit and M. Nakamura (private communication).